Aerial image quality control - spatial resolution

Ivar Oveland[1], Andreas Prebensen Korsnes[1], Eija Honkavaara[2], Lauri Markelin[2], Andrew C. Flatman[3], Henry Meißner[4,5]

[1] The Norwegian Mapping Authority, Kristiansand, Norway - ivar.oveland@kartverket.no, Andreas.Prebensen.Korsnes@kartverket.no
[2] NLS, Helsinki, Finland - eija.honkavaara@nls.fi, lauri.markelin@nls.fi
[3] KDS, Copenhagen, Denmark - anfla@kds.dk
[4] German Aerospace Center, Berlin, Germany - henry.meissner@dlr.de
[5] Geoinformatics and Land Management, OTH Amberg-Weiden, Amberg , Germany - h.meissner@oth-aw.de

Keywords: Siemens star, spatial resolution, ground sample distance (GSD), ground resolved distance (GRD), Aerial image, quality control.

Abstract

Standardized methods for assessing the spatial resolution of airborne photogrammetric systems are essential for ensuring consistent quality in aerial imaging. This study evaluates the use of Siemens stars for empirical estimation of Ground Resolving Distance (GRD) in high-altitude aerial photo missions, based on field experiments conducted in Norway and Denmark during 2023–2025. The results confirm a consistent and expected deviation between Ground Sampling Distance (GSD) and GRD, reinforcing GRD as a critical parameter for planning, procurement, and quality assurance in airborne photo missions. The study also shows that using external reference plates to obtain reliable black and white reference values improves the reliability of GRD estimations while simultaneously enabling using smaller Siemens star. This supports the use of the GRD method as a robust and practical framework for spatial resolution assessment in aerial imagery. The fundamental objective of the project is to establish common recommendations and methodologies for aerial image quality assessment, ultimately contributing to a European-wide GRD based resolution standard. Overall, structured and transparent GRD verification is necessary to ensure consistent quality in airborne optical imagery.

1. Introduction

Establishing a unified standard for aerial photography spatial resolution assessment is essential for ensuring consistent and comparable measurement practices across mapping and geospatial institutions. Such a standard would enable objective, reproducible measurements of spatial resolution, supporting reliable performance evaluations of aerial imaging systems (Meißner et al., 2019), (Meißner et al., 2018). For National Mapping and Cadastral Agencies (NMCAs), standardized resolving power assessment is particularly valuable, by allowing transparent benchmarking of different camera systems, informing mission planning, and optimizing efficiency and accuracy of photogrammetric mapping. By defining clear metrics and methodologies, the standard would improve procurement processes, foster innovation in remote sensing, and strengthen the reliability and usability of aerial imagery in both public and private sectors.

In 2024, a national survey conducted in Norway among professional users of aerial imagery revealed that ground resolution was the second most important quality criterion, cited by 84% of respondents. This result reinforces the need for a standardized approach focused on ground resolution as a core priority for mapping authorities across the Nordic region.

While Ground Sample Distance (GSD) describes nominal pixel spacing on ground, it does not reflect the true spatial detail captured. Ground Resolved Distance (GRD) accounting for the combined effects of sensor characteristics such as Bayer pattern interpolation, optical performance, atmospheric conditions, motion blur, and post-processing algorithms provides a more accurate measure. The Siemens star is one of the most effective tools for estimating GRD.

Evaluating the performance of an aerial photo mission campaign requires careful consideration of a wide range of variables, each of which can significantly influence the quality of the final images. Among the most critical quality indicators is the achieved GRD, which describes the smallest distinguishable details in the captured images. Variations in mission conditions and technical parameters can dramatically affect this metric. For systematic analysis, the most influential variables can be grouped into five categories: weather conditions, sensor design, camera settings, flight altitude, and post-processing workflows.

Weather conditions remain a fundamental external influence on image quality. Haze, humidity, sun angle, wind speed, and atmospheric turbulence can all reduce contrast or introduce geometric and radiometric distortions. Scattering from aerosols and molecules including dust and smoke has the potential to degrade GRD and limit the detectability of fine ground features.

Sensor design constitutes a critical technical factor that defines the intrinsic spatial and spectral characteristics of the acquired imagery. Different imaging architectures, including Bayer pattern colour filter array sensors and systems that use separate panchromatic and multispectral channels, vary significantly in both data acquisition and reconstruction processes. Bayer pattern sensors depend on demosaicing algorithms to reconstruct full-colour images from spectrally filtered sub-pixels. This reconstruction process can influence the final spatial fidelity of the imagery. Systems that combine a high-resolution panchromatic detector with lower-resolution multispectral channels rely on pansharpening techniques to merge spatial and spectral information. The performance of these pansharpening algorithms, together with the relative resolution differences and spectral response characteristics of the individual channels, has a substantial impact on the achievable GRD. Forward-motion compensation (FMC) mechanisms also play an essential role in preserving image sharpness. These mechanisms may be mechanical, electronic, or algorithmic in nature, and each aims to counteract the effects of platform motion and atmospheric disturbances during image acquisition. The effectiveness of FMC directly influences the degree of motion blur present in the imagery, and consequently, the level of spatial detail that can be reliably resolved.

Camera settings, such as shutter speed, aperture, ISO, and exposure strategy, also have direct impacts on image sharpness and noise levels. Proper configuration is required to balance illumination, motion compensation, and sensor limitations. Suboptimal settings may reduce image clarity, even if sensor design and environmental conditions are favourable.

Flight altitude directly determines the geometric scale and theoretical GSD of the imagery. Lower altitudes typically permit finer spatial resolution but may impose operational challenges such as reduced time for exposure and greater sensitivity to topographic variation. Higher altitudes may ease flight operations but increase atmospheric interference and potentially exceed the optical limits of the sensor. Thus, altitude selection involves balancing operational constraints against resolution requirements. In this study we define high altitude flight to be in the range from 2000 m to 3000 m above ground. It is common for optical airborne data acquisition to fly at a very high altitude that requires the aircraft to have a pressurized cabin (above 3000 m). This requires a glass plate in front of the camera to ensure that cabin pressure is maintained. Deformation in this glass plate as a result of pressure differences occurs. Additionally, any debris, oil and dirt on this plate can have an influence. Exhaust and heat from the aircraft’s engine can also have a degrading effect.

Post-processing workflows represent the final stage in which image quality may be enhanced, but the risk of degrading is present. Procedures such as radiometric calibration, noise reduction, geometric correction, sharpening, resampling, image compression and orthorectification must be conducted carefully to preserve spatial detail and avoid the introduction of artifacts.

The ultimate objective is to contribute to a common GRD-based resolution assessment framework for European NMCAs by proposing a structured procedure for GRD estimation and evaluation.

2. Methods and Materials

2.1 Practical implementation of GRD analyses in the NMCAs

The integration of the GRD estimation as a part of the aerial imagery quality control includes the following four major steps:

(1) Target Design and Scaling. The optimal size of the star is related to the target GSD being evaluated. Key design parameters include the star diameter and the number of black-white sectors, chapter 2.1.1.

(2) Siemens star material selection. The practical usability of a Siemens star also depends on its material and surface finish. Stars can be made from heavy rigid plates, fabric, or tarpaulin materials such as PVC vinyl or decotex fabric, chapter 2.1.2.

(3) GRD measurement algorithm and workflow. For reliable assessment of the MTF, tools such as DLR’s ”Resolving Power” tool (DLR, 2026) offer accessible and repeatable means to measure resolving power using Siemens star target, chapter 2.1.3.

(4) GRD analysis and interpretation. Analysis of the GRDs, considering the requirements of the output products, is essential to understand how GRD impacts the selected mapping tasks, chapter 2.2.1.

The following sections discuss each of these phases.

2.1.1 Target Design and Scaling:

The physical dimensions of the Siemens star target play a critical role in determining the Ground Resolving Distance (GRD). Large GSD requires large Siemens star, which is often difficult to deploy in the field.

Standardized recommendations have been established concerning the geometric design of Siemens star patterns (Meißner and Berger, 2025). The target is composed of alternating black and white radial sectors that gradually converge toward the center. Meißner and Berger tested the stability of the measured MTF values at different spatial frequencies (Meißner and Berger, 2025) for low altitude missions. Meißner and Berger tested frequencies from 8 to 48 Hz, corresponding to 16 and 96 total number of black and white segments. The result showed that all frequencies gave sufficiently robustness for practical application in low altitude airborne imaging missions.

Design guidelines for Siemens stars are derived from the requirement that pixels within each black and white sector remain independent at the maximum radius inside the star. Discussions are often related to the amount of pixels to ensure unaffected pixels. The designs shown in Figure 3 and 4 fulfil approximately 4.5 pixels at the outer part of the segment. Based on new development, the pixel count requirement has been challenged and tested (Meißner and Berger, 2025). The study has reduced the requirement to three pixels within a sector, which results in only one independent pixel remaining unaffected by the colour of adjacent sectors. This results in a dramatic reduction in the size of the Siemens star.

In additional to the three pixel demand a safety margin of 10% is recommended. These constraints together lead to the formulation expressed to estimate the recommended radius r for a Siemens star, in (equation 1) from (Meißner and Berger, 2025).

$$r = \frac{3 \cdot s \cdot GSD}{2\pi} + 0.1\left(\frac{3 \cdot s \cdot GSD}{2\pi}\right) \qquad (1)$$

Where s is the total number of black and white sections. Calculation for different frequencies are presented in Table 1, with GSD ranging from 0.05 m to 0.40 m.

A total of three different Siemens star designs were tested. The different designs are shown in Figure 1, 2, 3 and 4. Details about the star are summarized in Table 2 and 3.

2.1.2 Siemens star material selection:

Material selection of the Siemens star affects its usability: how easy or difficult the star is to transport and install to the ground, and how

	Total segments (white + black)			
GSD [m]	**16** (8Hz)	**24** (12Hz)	**32** (16Hz)	**96** (48Hz)
0.05	0.84	1.26	1.68	5.04
0.10	1.68	2.52	3.36	10.08
0.15	2.52	3.78	5.04	15.13
0.20	3.36	5.04	6.72	20.17
0.24	4.03	6.05	8.07	24.20
0.25	4.20	6.30	8.40	25.21
0.30	5.04	7.56	10.08	30.25
0.35	5.88	8.82	11.76	35.29
0.40	6.72	10.08	13.45	40.34

Table 1. Recomended siemens star diameter in meters at different GSD and number of segments, according to equation 1.

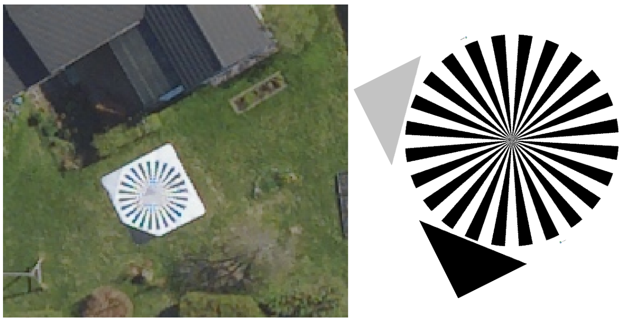

Figure 1. Siemens star design, Norway 2024.

Figure 2. Siemens star design, Norway 2025 multi colour.

Figure 3. Siemens star design, Norway 2025 DLR.

durable the star is against weather, wind, and time. Suitable materials for Siemens star can be similar to those that are used in different outdoor advertising banners. PVC and fabric materials are easy to pack for transportation, but they need to be secured firmly to the ground and as flat as possible. Rigid plates are stable, but more difficult to handle in larger sizes. If the fastening of the star to the ground requires wedges or spikes, the ground needs to be gravel, grass, or similar. If the ground is hard, such as asphalt, the star needs to be secured to the ground in some other means, such as external weights/stones.

Figure 4. Siemens star design, Denmark 2024 DLR.

Description	Figure	Total number of segments	Diameter (m)	New Eq.1 (m)
Norway 2024	1	48	4.05	5.04
Norway 2025 multi colour	2	24	4.00	2.52
Norway 2025 DLR	3	32	4.54	3.36
Denmark 2024 DLR	4	32	4.50	3.36

Table 2. Overview of the Siemens star designs used in this study, with the new diameter recommendation from Equation 1.

The following materials have been used in the Nordic countries, and the details are summarized in the following and in Table 3:

- Norway: The selected material was a PVC with a thickness of 500 g/m². This material is commonly used on commercial advertising banners. The material has widespread availability, suitability for large format printing, and is mechanically stable.

- Denmark: Different materials has been tested. In the latest version a matrix of Aluminum 3 mm plates was selected.

- Finland: Old star made of fabric (Honkavaara et al., 2006). The star (a semicircle) has 10º sectors and a 6.8 m radius. In this study only full circle siemens stars are used in the analyses. A new star, bought late 2025, is made of decotex-fabric with grey background, 24 Hz, 6m diameter with additional 2x2m black and white patches. Decotex is commonly used in commercial advertising banners and is available in various strengths. Both stars have metal rings and elastic band on their borders, so that the fabric can tighten to the ground as flat as possible using wedges/large spikes.

Description	Surface Material	Core material
Norway 2024	PVC	PVC 500 g/m²
Norway 2025 multi colour	PVC	PVC 500 g/m²
Norway 2025 DLR	PVC	PVC 500 g/m²
Denmark 2024 DLR	Plastic wrap	Aluminum, 3 mm

Table 3. Overview of the Material used in the siemens star.

2.1.3 GRD measurement algorithm and workflows: The GRD measurement algorithm and workflow based on the spatial frequency consists of three steps. First, the center of the Siemens star is determined using the method proposed by

Meißner and Berger (Meißner and Berger, 2025). Second, external colour reference patterns are measured to estimate the intensity levels corresponding to completely black and completely white surface. Alternately, when sufficiently large Siemens stars are used, the black and white reference levels can be derived automatically from the star itself. Third, after determining the center point, the GRD estimation method described by Meißner and Berger (Meißner and Berger, 2025) is applied. In this study, the reported GRD values were calculated as the average of the red, green, and blue colour channels. All analyses are performed in the software tool Resolving Power (1.0) (DLR, 2026).

2.2 Aerial image materials

An overview of the flight missions is provided in Table 4. In total, 12 flight missions are included in the study. Across these missions, 13 distinct flight lines and 59 aerial images contain a Siemens star. The imagery were acquired using five different camera systems and nine individual camera units. The Siemens stars were located at five different locations in Norway and Denmark.

Description	Total flight missions	GSD (m)	Camera
Norway 2024	2	0.1	Leica CountryMapper Leica DMC-4
Norway 2025 multi colour	1	0.1	Vexcel UltraCam Eagle M3
Norway 2025 DLR	2	0.1	Vexcel UltraCam Eagle M3
Denmark 2024 DLR	7	0.1	Ultracam Eagle M3 Ultracam Eagle Prime Leica DMC-4S

Table 4. Overview of the flight missions with corresponding camera system.

For the aerial photographic missions considered in this study, meteorological conditions were largely controlled. All missions were conducted under a clear blue sky, as this condition is a requirement to acquire high-quality imagery. Despite these variations in relative humidity and ambient temperature could still occur, potentially affecting image quality. Turbulence is expected to be minimal due to the relatively high flight altitudes employed, which reduces the likelihood of motion-induced blur and supports stable platform performance. Among technical and operational variables, the sensor design and flight altitude are known for all missions. Camera settings, such as shutter speed, aperture, ISO, and exposure strategy, were not systematically recorded, while post-processing methods applied to the imagery are also unknown.

2.2.1 GRD analysis and interpretation: The GRD is estimated for all images. This include finding the actual GSD. This is estimated using the position of the camera and the siemens star, pixels size of the camera's image sensor together with the focal length. The GRD is then found by dividing the GSD by the mean MTF 10 factor.

3. Result and Discussion

3.1 Analysis of image resolution

The presented method is used to calculate GSD and GRD. The result is presented in Figure 5 and shown together with the estimated distance between the camera position and the Siemens star, here called altitude. With in a flight lines the same Siemens star design is used. Flight line number 1-9 use Siemens star presented in Figure 4, while flight line number 12 and 13 use Siemens star presented in Figure 3.

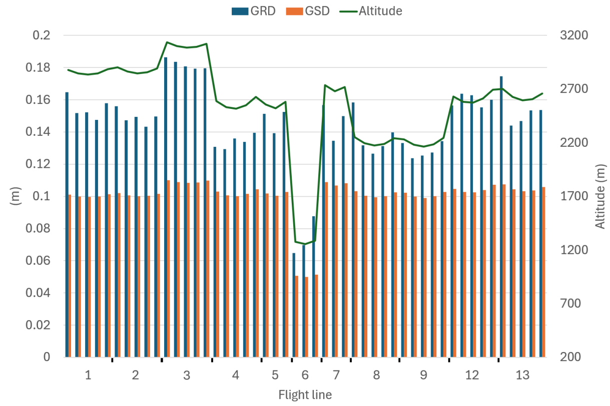

Figure 5. Estimated GSD, GRD for different flight lines. All lines use the same Siemens star presented in Figure 3 and 4 .

The analysis of image resolution is conducted by examining the ratio between GRD and GSD. The results are presented in Figure 6, together with the corresponding observation distance. The distance is defined as the distance from the camera to the Siemens star. Only images containing the Siemens star designs shown in Figures 3 and 4 are included in the evaluation. All flight lines were planned with a GSD of 0.10 m, except flight line 6, which was flown at a GSD of 0.05 m.

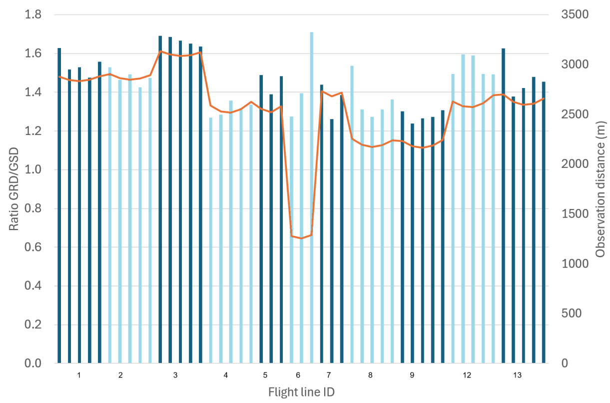

Figure 6. The ratio GRD/GSD calculated for the flight lines covering the Siemens star shown in Figure 3 and 4.

The observed patterns in the results can be grouped into three thematic insights. The first relates to the correlation between flight altitude and the resulting GRD/GSD ratio. The second concerns the variation observed within individual flight lines. Each flight line contains several images covering the Siemens star, and the star appears at different positions within the image frame. This positional variation may introduce differences related to image homogeneity in hence of GRD. Camera design can play an important role for this topic. Sensors based on Bayer-pattern demosaicing typically exhibit stronger pixel level coupling, while pan sharpened systems merge information from multiple cameras, potential resulting in different spatial homogeneity characteristics. The third theme concerns the expected performance of high altitude optical airborne data acquisition. A clear discrepancy is observed between the nominal GSD and the effective GRD achieved in practice.

In the presented results, the ratios are linked to flight line numbers rather than specific camera instruments. This choice is motivated by the substantial variability between flight missions, which makes it difficult to isolate individual error sources or attribute differences to specific camera units.

To illustrate this, we examine flight lines 12 and 13. Both flight lines were captured using the same camera system (identical serial number), flown at the same altitude, and using the same Siemens star target. The only differences between them are the acquisition date, geographic location, and post processing colour settings. The average GRD/GSD ratios for the two flight lines are 1.53 and 1.47, respectively.

3.2 Influence of Siemens star size on GRD estimation

In this study a simulation of different Siemens star sizes is performed. This is done by calculating the GRD using different diameter of the Siemens star as shown in Figure 7. The calculation starts at the smallest possible diameter where the software is able to calculate a result. Similar, the diameter increment and calculations stops at the largest possible diameter.

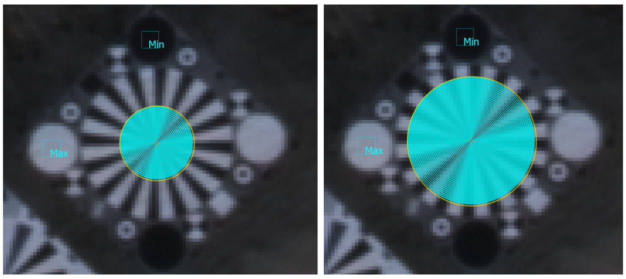

Figure 7. To the left the GRD calulation is performed with data within a dimaeter of 2.26 m. Simular to the left a dimatere of 3.90 m.

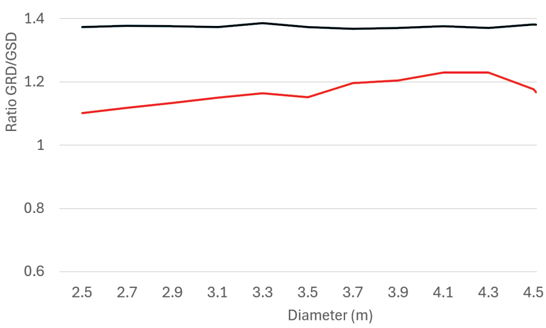

Figure 8. The ratio between the GRD and GSD calculations with different Siemens star diameter simulations. The black curve shows the result with external reference plates and the red curve is without reference using reference pixels from within the star.

The result of the Siemens star size simulation is shown in Figure 8. The evaluation is done on pansharpened uncompressed 8 bit image and is based on the average GRD result of red, green and blue colour band. The GSD is calculated using the Siemens star and camera position. The GRD is calculated using two different methods to represent pure black and white values. The first use black and white reference pixel values derived from external plates. The second method use black and white reference pixel derived from within the Siemens star, using the widest part of the sectors.

When using reference pixel values from external plates, the GRD/GSD ratio remains stable at slightly below 1.4 for Siemens star diameters ranging from 2.5 to 4.5 m, indicating reliable measurements across this range. The result shows that the GRD/GSD ratio is stable with a significantly smaller diameter than the Siemens star used in this simulation, shown in Figure 3. When using reference pixel values from the widest sectors, the GRD/GSD ratio varies with the Siemens star diameter and remains significantly lower than when reference values are obtained from external plates. This indicates that the sector-based reference pixels do not represent pure black and white values.

The recommended star diameter presented by Meißner and Berger (Meißner and Berger, 2025) and Equation 1 is 3.4 m. The simulation indicates that the diameter recommendations provide a stable result when external colour reference patterns are used. The size of the external reference is important in the GRD calculations. It is important that the size is sufficient to get a clear black and a clear white pixel. In the flight missions with the description ”Norway 2024” the size of the black reference was to small, as shown in Figure 9. All GRD calculation in this study are made with external reference pattern. Due to this the ”Norway 2024” flight mission is excluded in the analyses in this study.

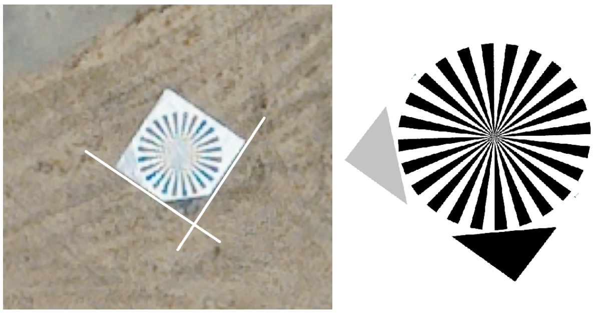

Figure 9. Example where the black external colour reference patterns is to small.

The various external black reference targets are summarized in Table 5, along with the corresponding number of pixels contained within each reference. The number of pixels are based on a GSD of 0.1 m. Table 5 also differentiates between pixel counts obtained prior to image enhancement and those resulting from demosaicing (factor 2) and pan-sharpening procedures (factor 3). The results indicate that an external black reference pattern should exceed nine pixels in size to ensure compatibility with cameras commonly employed in remote sensing missions.

3.3 Analysis of processing and measurement effects

Aerial imagery is typically characterized by very large file sizes, primarily due to the high number of pixels required for photogrammetric and remote-sensing applications. To manage storage and facilitate efficient data handling, image compression is routinely applied. Compression practices vary between countries. In Norway a standard compression is JEPG with compression factor of Q97 and Q95, while Denmark uses a compression factor of Q90. Figure 10 illustrates the relationship between compression level, number of spectral bands, and resulting file size. The results are derived from a representative

Description	Diameter external reference	Nr. of pixels before image enhancment	Nr. of pixels in final image
Norway 2024	0.91 m	4.6	9.1
Norway 2025 multi colour	0.85 m	2.8	8.5
Norway 2025 DLR	1.44 m	4.8	14.4
Denmark 2024 DLR	1.43 m	7.2	14.3

Table 5. Size of external reference pattern in the different Siemens star designs with corresponding number of pixels with GSD 0.1 m.

pansharpened aerial image from Norway and demonstrate the substantial reduction in storage requirements achieved through different JPEG compression settings.

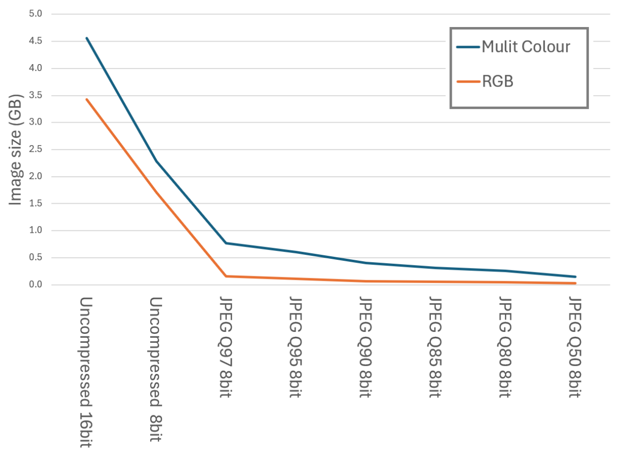

Figure 10. The effect in image file size for different number of colur bands and JEPG compression factors.

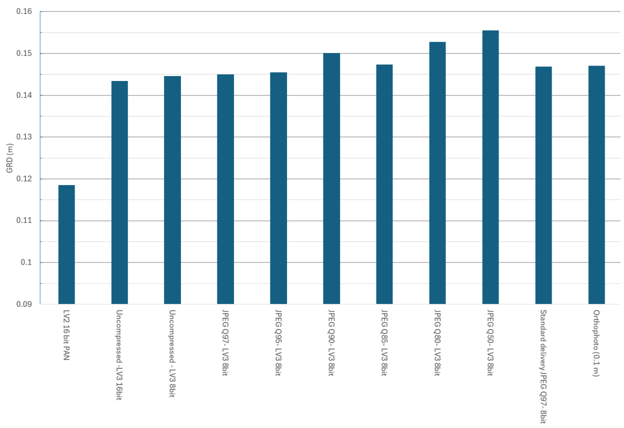

Figure 11. The average GRD result of red, green and blue colour band calculations with difference image compressions.

Figure 11 shows the average GRD result of red, green and blue colour bands calculated from the same image with different JPEG compressions with measurements of external colour reference patterns for black and white. The image is collected from flight line 13. GRD does not change significantly with JPEG compressions that are used in Norway (quality factor 97 and 95) compared to an uncompressed version of the same image.

3.4 Recommendations and further steps

Based on the analysis, the following conclusions and recommendations for further work can be drawn. The GRD values do not change significantly with Siemens star sizes larger than the recommended sizes in Equation 1. This requires measurement of external colour reference patterns for black and white in the calculation. A smaller star simplifies the transport, storage and handling of the Siemens star. For PVC banners it is recommended to roll and not fold the PVC banner during transportation and storage. This is important to prevent creases on the banner that cannot be straightened out. An important safety feature when handling large PVC banners is to avoid tying the banner to objects that could move if the banner is caught in the wind. GRD varies between images within a flight line. Consequently, we recommend measuring all images that contain the Siemens star to capture all possible measurements within a project. The resulting values can then be compared with the specified requirements, for example using maximum and/or average GRD.

An alternative method to reduce the physical size of Siemens star is to reduce the circle from a full circle to a segment of a circle. This approach could be more vulnerable for blurring in flight direction caused by forward motion compensation, exposer time and velocity. Further study is needed to get a full understanding of the risk associated with this along with the reduction in compliance in MTF calculations this will entail.

To continue this study the following research questions needs to be continued and supported with more data and Siemens star design:

1. How well does GRD represent the effective spatial resolution of aerial imagery compared to nominal GSD under operational conditions?
2. How do key factors, such as sensor design, flight altitude, and image position affect GRD and its relationship to GSD?
3. To what extent does the size and design of the Siemens star influence the reliability and robustness of GRD estimation?
4. How do processing steps, including orthophoto generation and image compression, affect GRD estimates of final products?
5. How can GRD estimation be structured into a practical and standardized workflow for quality assurance and quality control in aerial imaging?

4. Conclusion

This study evaluates the use of Siemens stars in Norway and Denmark during 2023-2025. The results demonstrate a significant and expected difference between ground sample distance (GSD) and ground resolved distance (GRD), highlighting that the GRD is a critical parameter when planning and procuring aerial imagery services. GRD relates to the smallest objects that can be reliably mapped. Incorporating GRD into planning ensures that expectations match the final outcome and end product. This study provides valuable insight into the practical use of Siemens stars considering size, frequency, design, material selection and images compression.

The findings indicate that the results presented in (Meißner and Berger, 2025) also apply to high altitude pansharpened aerial missions, meaning that the Siemens star can be reduced in size accordingly, provided that external reference plate is used. In this study, reliable GRD estimations were obtained using a Siemens star with a 2.5 m diameter and the reference plates for pure black and white pixels.

The Nordic countries apply different strategies for GSD evaluation, ranging from prequalification to national calibration sites and field installations on individual projects. The study has shown that it is possible to reduce the size of the Siemens star. This makes it more doable to provide Siemens star capabilities within the project area. It remains unclear whether the best solution is national calibration site compared to Siemens star in every project. Important factors to consider are the size of the country, infrastructure within the project area, and accessibility.

The study did not include enough data to determine differences between camera types, primarily due to the large number of variables. One tendency observed, however, is a correlation between the GRD/GSD ratio and flight altitude. Additional, image compression down to JPEG Q95 has only minor effects on GRD. However, the results highlight that post processing steps such as colour adjustments, and orthophoto generation do influence the GRD of the final products. Careful attention to post processing workflows is therefore essential to achieve an optimal GRD/GSD ratio. Further studies will collect additional data from different European countries to support the development of a standardized European framework for aerial image resolution assessment. These datasets will also be used to derive further conclusions on factors influencing image resolution.

The GRD method used and presented in this study represent a practical and theoretically grounded framework for evaluating the spatial resolution in an aerial image. The project aims to establish common requirements and methodologies for aerial image quality assessment, ultimately contributing to a European-wide GRD based resolution standard. Overall, structured and transparent GRD verification is necessary to ensure consistent quality in airborne optical imagery.

5. Acknowledgements

The authors acknowledge Geovekst (Norway) for financing the Siemens stars and aerial images taken in Norway. We also thank Steinar Kjellevik Karlsen and Pål Tanem for their administration and logistical support during the fieldwork related to the Siemens stars in Norway.

During the development of this manuscript, the authors used ChatGPT and Copilot to improve the readability and language of the text. The authors have reviewed the content and assume full responsibility for the final published article.

References

DLR, 2026. Website german aerospace center (DLR), resolving power. https://macs.dlr.de/box/resolvingpower/resolvingpower_en.html. Accessed: 2026-05-22.

Honkavaara, E., Jaakkola, J., Markelin, L., Becker, S., 2006. Evaluation of resolving power and MTF of DMC. *International Archives of Photogrammetry, Remote Sensing and Spatial Information Sciences*, 36(6).

Meißner, H., Berger, R., 2025. Adaptable Siemens Star Targets for Reliable and Standardized Spatial Resolution Measurement under DIN 18740-8. *The International Archives of the Photogrammetry, Remote Sensing and Spatial Information Sciences*, 48, 139–146.

Meißner, H., Cramer, M., Reulke, R., 2018. Towards standardized evaluation of image quality for airborne camera systems. *The International Archives of the Photogrammetry, Remote Sensing and Spatial Information Sciences*, 42, 295–300.

Meißner, H., Cramer, M., Reulke, R., 2019. Evaluation of structures and methods for resolution determination of remote sensing sensors. *Pacific-Rim Symposium on Image and Video Technology*, Springer, 59–69.